Chinese Chemical Letters 35 (2024) 109602

Contents lists available at ScienceDirect

Chinese Chemical Letters

journal homepage: www.elsevier.com/locate/cclet

A β-lactamase-activatable photosensitizer for the treatment of resistant bacterial infections

Zhipeng Li[a], Qincong Feng[a], Jianliang Shen[a,b,*]

[a] National Engineering Research Center of Ophthalmology and Optometry, Eye Hospital, Wenzhou Medical University, Wenzhou 325027, China
[b] Zhejiang Engineering Research Center for Tissue Repair Materials, Wenzhou Institute, University of Chinese Academy of Sciences, Wenzhou 325001, China

ARTICLE INFO

Article history:
Received 6 December 2023
Revised 28 January 2024
Accepted 29 January 2024
Available online 6 February 2024

Keywords:
Activatable photosensitizer
MRSA
β-Lactamase
Fluorescence imaging
aPDT

ABSTRACT

Antibacterial agent of activatable photosensitizer not only has the advantages of traditional photosensitizers, such as good curative effect and low resistance, but also has better selectivity for bacteria and lower toxicity to normal tissues. Limited reports of activatable photosensitizer can be used to treat drug-resistant bacteria. In order to meet this challenge, we designed and synthesized an activatable photosensitizer (**Ce-OHOA**), which can not only selectively identify methicillin-resistant *Staphylococcus aureus* (MRSA) with high expression of β-lactamase by fluorescence imaging, but also kill MRSA with less than 10 times the concentration and 10 times the irradiation dose of CySG-2 reported. **Ce-OHOA** not only combines the dual functions of fluorescence diagnosis and photodynamic therapy, but also selectively acts on bacteria with high expression of β-lactamase and has little toxicity to normal cells. We expect that the study of this activating photosensitizer will provide a new solution for antibacterial photodynamic therapy (aPDT) of drug-resistant bacteria.

β-Lactam antibiotics are antibiotics that contain a β-lactam structure in their molecules [1]. This class of antibiotics is the most widely used and has several advantages, including strong bactericidal activity, low toxicity, wide indications, and good clinical efficacy [2,3]. However, the widespread use of these antibiotics inevitably leads to the emergence of drug-resistant bacteria, resulting in reduced therapeutic efficacy and other issues [4,5]. β-Lactamase, also known as cephalosporinase or penicillinase (E.C.3.5.2.6), is a zinc ion-dependent amide hydrolase that degrades penicillin antibiotics, such as penicillin G [6,7]. The destruction of β-lactam antibiotics' structure by bacteria, due to the high expression of β-lactamase, is considered one of the most common mechanisms of bacterial resistance. Therefore, the development of diagnostic and therapeutic reagents that target β-lactamase is of great significance in addressing bacterial resistance [8,9].

Antimicrobial photodynamic therapy (aPDT) is a novel of antimicrobial method that utilizes a light source and photosensitizer (PS) to eradicate bacteria [10]. The principle of this technology is that PSs are activated by specific wavelengths of light to produce reactive oxygen species (ROS) molecules. These molecules rapidly oxidize bacterial lipids and proteins, leading to the destruction of the bacterial membrane structure and initiating cell death [11]. PS shows high broad-spectrum bactericidal activity and can effectively kill gram-positive, gram-positive bacteria or drug-resistant bacteria [12]. In aPDT, the PS is the key factor. A number of small molecule antimicrobial PSs have been developed, and many of them demonstrate strong bacterial inhibition at the nanomolar level [13–18]. However, most PS does not possess targeting properties, as a result, they will inevitably cause damage to the surrounding normal cells while targeting the bacteria [19]. The emergence of activatable PSs effectively solves the targeting issue associated with conventional PSs. Before being activated by a specific biological microenvironment, the fluorescence and photodynamic effects of activatable PS are weak. After activation, the fluorescence and photodynamic effects of the PS are enhanced [20–22]. At present, most of the activatable PSs are primarily used in antitumor research, with fewer reports on their use in antibacterial applications [23–31]. Therefore, the development of activatable PSs for precise anti-drug-resistant bacteria therapy is crucial.

Several near-infrared activatable antimicrobial PSs have been reported to offer significant advantages in terms of wavelength and depth of penetration. However, the core of the PSs used in these studies has low single-linear oxygen ($^1O_2$) yields [32,33]. This necessitates higher concentrations and light doses for antimicrobial activity. 4–Hydroxyl–oxoisoaporphine (OHOA), which was first reported by Xu *et al.*, stands out due to its high fluorescence

* Corresponding author.
E-mail address: shenjl@wiucas.ac.cn (J. Shen).

https://doi.org/10.1016/j.cclet.2024.109602
1001-8417/

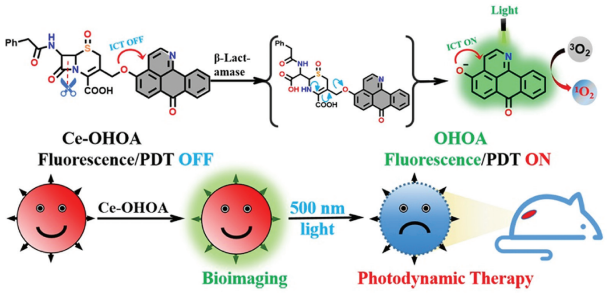

Scheme 1. Illustration of **Ce-OHOA** for selective imaging and photodynamic antibacterial.

quantum yield (0.72 in phosphate buffer saline (PBS)), high $^1O_2$ yield (0.06), and low cytotoxicity [34]. Despite its excellent performance as a PS, OHOA has not been previously designed to be an activatable PS. In this study, we synthesized an activated PS called **Ce-OHOA** by connecting the OHOA and cephalosporin structures using ether bonds. **Ce-OHOA** exhibits a low fluorescence quantum yield and a $^1O_2$ yield. However, when it undergoes hydrolysis by β-lactamase, OHOA with high fluorescence quantum yields and high $^1O_2$ yields is generated. Experimental results *in vitro* and *in vivo* showed that **Ce-OHOA** could not only be used for fluorescence imaging of methicillin-resistant *Staphylococcus aureus* (MRSA) with high expression of β-lactamase enzymes, but also exhibited excellent photodynamic antimicrobial effects both *in vivo* and *in vitro* (Scheme 1).

OHOA was synthesized using previously reported literature methods [34]. The probe **Ce-OHOA** consisted of OHOA and Ce-Cl, and the complete synthesis procedure of **Ce-OHOA** is shown in Scheme S1 (Supporting information). The structure of **Ce-OHOA** and its intermediates were found to be unstable on silica gel and could not be effectively separated using conventional column chromatography to obtain pure products. Therefore, the products obtained during the synthesis step were purified using pulping. **Ce-OHOA** was characterized by ^{1}H nuclear magnetic resonance (NMR), ^{13}C NMR, and high resolution mass spectroscopy (HRMS) analyses (Figs. S1–S4 in Supporting information). The basic photophysical properties of **Ce-OHOA** and OHOA in PBS buffer are listed in Table S1 (Supporting information).

Fig. 1A shows the absorption spectra of **Ce-OHOA** (blue) and **Ce-OHOA** + β-lactamase (red). The maximum absorption position of **Ce-OHOA** shifted from 410 nm to 476 nm before and after reacting with β-lactamase. In addition, the fluorescence emission spectrum of **Ce-OHOA**, when reacted with β-lactamase, exhibited a significant enhancement under 480 nm light excitation. The maximum emission intensity (I_{535}) was observed at 535 nm (Fig. 1B). We next measured the appropriate pH and temperature for the reaction of **Ce-OHOA** with β-lactamase, as shown in Fig. S5A (Supporting information). The fluorescence intensity of **Ce-OHOA** in different pH environments before **Ce-OHOA** did not interact with the enzyme was consistently low. The fluorescence of **Ce-OHOA** after interaction with β-lactamase, varied significantly in different pH environments, with the highest intensity observed at pH 7.4. In the temperature-dependent experiments (Fig. S5B in Supporting information), the fluorescence intensity of **Ce-OHOA** remained low at 25–40 °C before interacting with β-lactamase. After interacting with β-lactamase, the fluorescence intensity of **Ce-OHOA** was the strongest at 37 °C. Therefore, we chose to study the reaction of **Ce-OHOA** with β-lactamase at 37 °C and pH 7.4. The fluorescence intensity of **Ce-OHOA**, which is time-dependent, shows a rapid increase with different amounts of β-lactamase (Figs. 1C–E). However, after approximately 60 min, the rate of increase in fluorescence intensity decreases. In addition, there was a good linear relationship between the intensity and β-lactamase concentration within the range of 0–64 nmol/L. A limit of detection (LOD) of 0.83 nmol/L was determined (Fig. 1F). To specifically detect the **Ce-OHOA** interacting by β-lactamase, the fluorescence intensity at 535 nm was measured. The selectivity of **Ce-OHOA** was tested, and the results in Fig. S6 (Supporting information) show that **Ce-OHOA** is not interfered with by other analytes. In order to investigate the recognition mechanism of **Ce-OHOA** with β-lactamase, **Ce-OHOA** was co-incubated with β-lactamase (64 nmol/L) for 60 min and the products after the reaction were monitored by high performance liquid chromatography (HPLC). At the end of the reaction, a new peak was observed at 2.29 min, which had a retention time (Rt) consistent with that of OHOA (Rt = 2.29 min). In contrast, the peak of **Ce-OHOA** at 4.72 min decreased in size (Fig. S7 in Supporting information). Mass spectrometry showed that the molecular weight of the peak with retention time of 2.29 min was consistent with OHOA (Fig. S8 in Supporting information) [35]. HPLC analysis showed that **Ce-OHOA** could be hydrolyzed by β-lactamase to produce OHOA.

In order to gain a clearer understanding of the interaction between **Ce-OHOA** and β-lactamase probes, we employed molecular docking software. As shown in Fig. S9A (Supporting information), the carboxyl group and the carbonyl group of the amide bond in the structure of **Ce-OHOA** form multiple sets of hydrogen bonds with Ala237, Ser70, Ser130, Ser235, and Ser244 of β-lactamase to achieve precise recognition. The distance between the hydroxyl group of Ser70, which plays a catalytic role in the β-lactamase, and the carbonyl carbon atom of the **Ce-OHOA**'s lactam ring is only 0.32 nm. This close proximity ensures that the hydrolysis of the amide bond proceeds normally. In order to investigate the luminescence mechanism of **Ce-OHOA** after hydrolysis by β-lactamase, we utilized the calculated molecular orbital energies of **Ce-OHOA** and OHOA. As shown in Fig. S9B (Supporting information), the energy level difference between the highest occupied molecular orbital and the lowest unoccupied molecular orbital of **Ce-OHOA** is 3.38 eV, which is higher than that of OHOA (2.83 eV). Therefore, **Ce-OHOA** requires a higher energy of light for excitation. When **Ce-OHOA** is irradiated with 500 nm light, it does not undergo intramolecular charge transfer (ICT) due to insufficient light energy, resulting in weak luminescence [36]. When 500 nm light is used to irradiate OHOA, the ICT occurs easily and it exhibits strong luminescence.

Subsequently, time-dependent MRSA imaging experiments were conducted. As shown in Fig. S10 (Supporting information), a weak green fluorescence emission appeared after 20 min of incubation of **Ce-OHOA** with MRSA, reaching its brightest at 60 min. Therefore, 60 min was chosen as the optimal time for bacterial fluorescence imaging. As shown in Fig. 2, the fluorescence signal of MRSA was significantly weakened after treating with potassium clavulanate (PC) compared to the untreated group. The same weakening of the fluorescence signal was also observed in *S. aureus*, which expresses a lower level of β-lactamase. The above results suggest that the fluorescent signal in bacteria is generated through the specific recognition of **Ce-OHOA** by β-lactamase.

In order to minimize the false damage of photosensitizers to normal tissues, **Ce-OHOA** was designed as an activatable type. The release of $^1O_2$ was detected by monitoring the absorption at 400 nm using the commercial dye ABDA. The results showed that at 500 nm light emitting diode (LED), **Ce-OHOA** hardly produced $^1O_2$ without β-lactamase activation (Fig. S11A in Supporting information). After treatment with β-lactamase, the absorption of ABDA at 400 nm was reduced by approximately 57% (Fig. S11B in Supporting information). This demonstrates that **Ce-OHOA** can release large amounts of rapidly $^1O_2$ for antimicrobial use only after selective activation by β-lactamase.

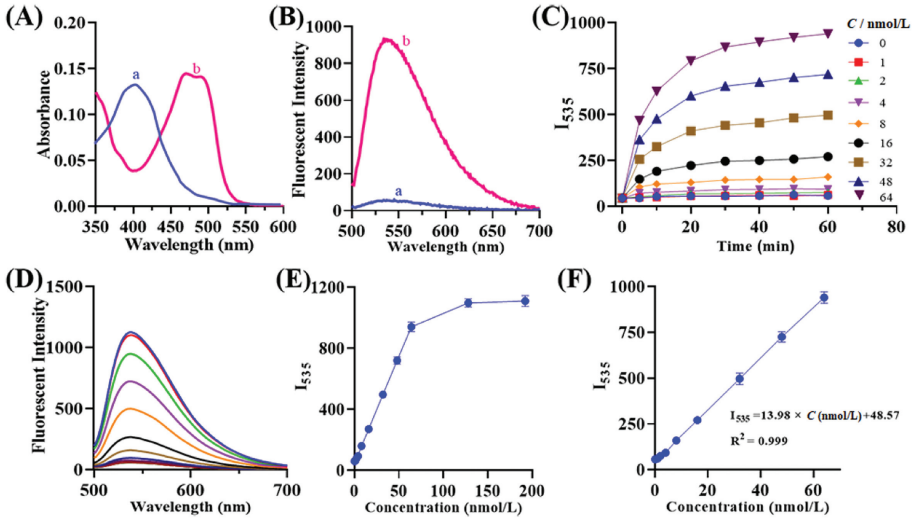

Fig. 1. (A) Absorption and (B) fluorescence emission spectra of **Ce-OHOA** (10 μmol/L) before (a) and after (b) reaction with β-lactamase (64 nmol/L) at 25 °C for 30 min in PBS (pH 7.4). λ_{ex} = 480 nm. (C) Plots of fluorescence intensity I_{535}. The reaction time of **Ce-OHOA** (10 μmol/L) with varied concentrations of β-lactamase (0–64 nmol/L). λ_{ex} = 480 nm. (D) Fluorescence emission spectra of **Ce-OHOA** (10 μmol/L) with 0–192 nmol/L β-lactamase. (E) Fluorescence intensity I_{535} of **Ce-OHOA** (10 μmol/L) with 0–192 nmol/L β-lactamase. (F) Linear fitting curve of fluorescence intensity I_{535} toward the concentration of β-lactamase (0–64 nmol/L). λ_{ex} = 480 nm.

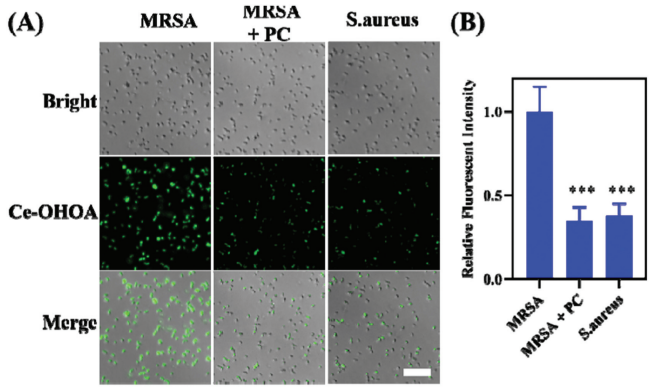

Fig. 2. (A) Confocal fluorescence images of MRSA, MRSA+PC and *S. aureus* (non-expressing β-lactamase) incubated with **Ce-OHOA** (10 μmol/L). Scale bar: 20 μm. (B) Relative pixel intensity of the corresponding fluorescence images in pane A. $^{***}P < 0.001$ *vs.* MRSA group. Error bars: mean ± standard deviation (SD) ($n = 10$).

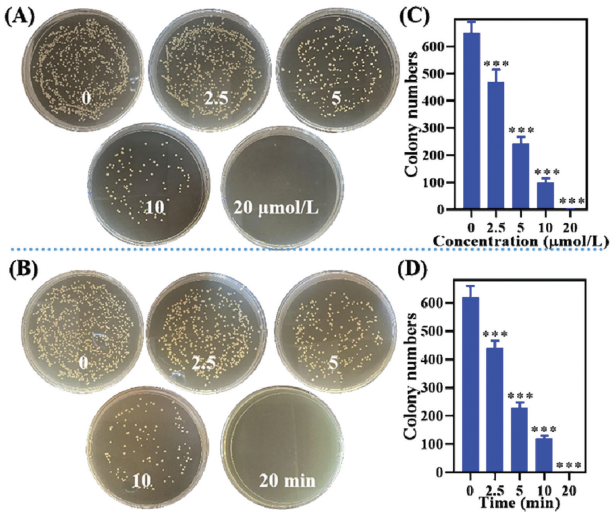

Fig. 3. Digital images of clonogenic assay performed in plates, with clones produced by MRSA under different concentrations (A) or different illumination times (B). (C, D) Colony numbers are counted using Image J. All the data are presented as mean ± SD ($n = 3$). $^{***}P < 0.001$ *vs.* control group.

We then investigated the PDT effect of **Ce-OHOA** on MRSA. We conducted a series of experiments to investigate the concentration-dependent and light dose-dependent photoinactivation effects of **Ce-OHOA** against MRSA. In the concentration-dependent group, different concentrations of **Ce-OHOA** were cultured with MRSA for 60 min, then irradiated with or without LED. In the non-LED group (Fig. S12 in Supporting information), the survival of MRSA decreased with increasing **Ce-OHOA** concentration, but even at concentrations as high as 100 μmol/L, the survival rate of MRSA survival remained above 60%. In the LED group (Fig. 3), the survival rate of MRSA gradually decreased as the concentrations of **Ce-OHOA** increased. When the concentration of **Ce-OHOA** was only 2.5 μmol/L, the survival rate of MRSA decreased significantly to 74.6%. However, when the concentration of **Ce-OHOA** was increased to 20 μmol/L, the survival rate dropped to only 0.1% (Figs. 3A and C). In the light dose-dependent group (Figs. 3B and D), the survival rate of MRSA decreased significantly and gradually with the increase in light dose. The survival rate of MRSA significantly decreased to 72.1% at 2.5 min, and only 0.1% at 20 min. These results indicate that **Ce-OHOA** has a strong bactericidal effect on MRSA strains that exhibit high expression of β-lactamase under light conditions, and its antibacterial concentration and light dose are obviously lower than those reported activatable photosensitizer (Table S2 in Supporting information).

Diamidino-2-phenylindole (DAPI) and propidium iodide (PI) co-staining was used to study the mechanism of bacterial death. As depicted in Fig. S13 (Supporting information), when the MRSA were incubated with **Ce-OHOA** without light irradiation, only blue fluorescence (DAPI) was observed in the bacteria. However, under the light condition, both blue fluorescence (DAPI) and red fluorescence (PI) was observed in the bacteria. DAPI stains bacteria with intact cell membranes, while PI only stains bacteria with damaged cell membranes [14]. This suggesting that the bacteria incubated with the **Ce-OHOA** experienced damage to their cell membranes of under light conditions, potentially leading to their death.

The favorable *in vitro* antimicrobial effect of **Ce-OHOA** prompted us to further investigate its effect *in vivo* using aPDT. We chose a rat wound model to study the antimicrobial potential of **Ce-OHOA**. To assess the safety of **Ce-OHOA** at the infection site in rats, we

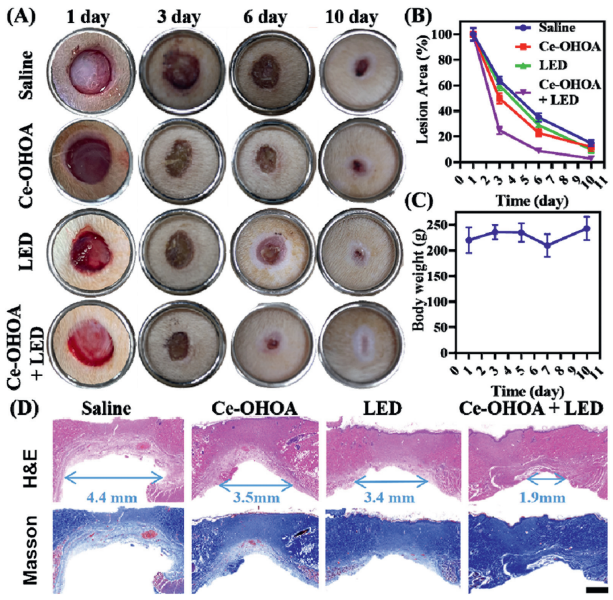

Fig. 4. *In vivo* antibacterial evaluation of **Ce-OHOA** for MRSA-infected wounds of Rat. (A) Successive photographs of wounds without and with aPDT treatment. Inside diameter of stainless-steel ring = 16 mm. (B) Time-dependent lesion area. (C) Body weight change of rats. (D) H&E staining and Masson staining images of the sectioned tissues of wounds without and with aPDT treatment on day 10 post-infection. Scale bar: 1.0 mm. Error bars: mean ± SD ($n = 4$).

initially examined the photo/dark toxicity of **Ce-OHOA** on RS1 cells (rat skin fibroblast cell line). As demonstrated in Fig. S14 (Supporting information), **Ce-OHOA** showed good biocompatibility with RS1 cells, with cell survival remained above 85% even under light conditions when the concentration was below 40 μmol/L.

After demonstrating the favorable biocompatibility of **Ce-OHOA** with normal skin, we conducted additional photodynamic antimicrobial validation using a rat wound infection model (Adherence to the ethical standards set by the Animal Ethics Committee at Wenzhou Medical University was ensured, approval number: Wydw7019–0134). As depicted in Figs. 4A and B, the rate of wound healing was slower in the saline, saline + LED, and **Ce-OHOA** groups when compared to the **Ce-OHOA** + LED group. On day 10, the infected wound form the **Ce-OHOA** + LED group only slight marks, while all other control groups showed varying degrees of unrepaired wounds. Under the irradiation of the 500 nm LED, the rats did not show any recurrence of the wound or signs of septic infection. Moreover, the body weight of rat fluctuated within the normal range during the treatment (Fig. 4C), indicating that **Ce-OHOA** accelerates the healing of infected wounds through antibacterial photodynamic therapy.

The therapeutic efficacy was further examined by performing hematoxylin-eosin staining (H&E) staining and Masson staining on day 10 after infection. As illustrated in Fig. 4D, H&E histological analysis showed that **Ce-OHOA** plus irradiation resulted in shorter mean length of granulation gap and the formation of thicker epithelial tissue with improved histological architecture compared to the other three groups. Masson staining showed an organized arrangement of collagen. These results strongly indicate that **Ce-OHOA** plus LED irradiation has a significant advantage in suppressing MRSA infections and promoting wound healing.

In this paper, we developed an activatable photosensitizer (**Ce-OHOA**) against MRSA with high expression of β-lactamase. **Ce-OHOA** not only shows good sensitivity and high anti-interference ability to β-lactamase in aqueous solution, but also can image the MRSA with high expression of β-lactamase *in vitro*. In addition, *in vitro* and *in vivo* antibacterial experiments, **Ce-OHOA** showed a strong antibacterial effect at low light dose (12 J/cm^2) and low concentration (10 μmol/L), and contributed to the wound healing of MRSA-infected animal models. Overall, **Ce-OHOA** is outstanding in fluorescence detection and photodynamic antibacterial function. Such rationally designed activatable photosensitizer will provide a new idea for the study of diagnostic and therapeutic reagents for drug-resistant bacteria.

Declaration of competing interest

The authors declare that they have no known competing financial interests or personal relationships that could have appeared to influence the work reported in this paper.

Acknowledgments

This work was financially supported by the National Natural Science Foundation of China (No. 21977081), Zhejiang Provincial Natural Science of Foundation of China (No. LQ21H190006).

Supplementary materials

Supplementary material associated with this article can be found, in the online version, at doi:10.1016/j.cclet.2024.109602.

References

[1] E. Minaldi, E.J. Phillips, A. Norton, Clin. Rev. Allergy Immunol. 62 (2022) 449–462.
[2] C.L. Tooke, P. Hinchliffe, E.C. Bragginton, et al., J. Mol. Biol. 431 (2019) 3472–3500.
[3] L.M. Lima, B.N.M. da Silva, G. Barbosa, et al., Eur. J. Med. Chem. 15 (2020) 112829.
[4] M.L.M. Salverda, J.A.G.M. De Visser, M. Barlow, FEMS Microbiol. Rev. 34 (2010) 1015–1036.
[5] J. Li, W. Sun, Z. Yang, G. Gao, et al., ACS Appl. Mater. Interfaces 12 (2020) 54378–54386.
[6] E. Dellus-Gur, M. Elias, E. Caselli, F. Prati, et al., J. Mol. Biol. 427 (2015) 2396–2409.
[7] M.F. Mojica, M.-A. Rossi, A.J. Vila, et al., Lancet Infect. Dis. 22 (2022) 28–34.
[8] Z. Yi, X. Xu, X. Meng, et al., Chin. Chem. Lett. 34 (2023) 108238.
[9] H. Zhang, C. He, L. Shen, et al., Chin. Chem. Lett. 34 (2023) 108160.
[10] S.P. Songca, Y. Adjei, Int. J. Mol. Sci. 23 (2022) 3209.
[11] F.F. Sperandio, Y.Y. Huang, M.R. Hamblin, Drug Disc. 8 (2013) 108–120.
[12] H.R. Jia, Y.X. Zhu, Z. Chen, F.G. Wu, ACS Appl. Mater. Interfaces 9 (2017) 15943–15951.
[13] N. Vn, Z. Z, T. Bz, Y. J, Chem. Soc. Rev. 51 (2022) 3324–3340.
[14] G. Lin, M. Hu, R. Zhang, et al., J. Med. Chem. 64 (2021) 18143–18157.
[15] E. Caruso, S. Banfi, P. Barbieri, et al., J. Photochem. Photobiol. B 114 (2012) 44–51.
[16] F. Hu, S. Xu, B. Liu, Adv. Mater. 30 (2018) e1801350.
[17] E. Zhao, Y. Chen, H. Wang, et al., ACS Appl. Mater. Interfaces 7 (2015) 7180–7188.
[18] S. Wang, W. Wu, P. Manghnani, et al., ACS Nano 13 (2019) 3095–3105.
[19] E. Caruso, S. Ferrara, P. Ferruti, et al., Lasers Med. Sci. 33 (2018) 1401–1407.
[20] Y. Wen, N. Jing, M. Zhang, et al., Adv. Sci. 10 (2023) e2206681.
[21] X. Li, F. Huo, Y. Zhang, F. Cheng, et al., J. Mater. Chem. B 10 (2022) 5504–5519.
[22] X. He, Z. Zheng, F. Zhang, et al., ACS Appl. Bio Mater. 3 (2020) 7886–7897.
[23] Z. Li, Q. Feng, J. Hou, et al., Bioorg. Chem. 143 (2023) 107021.
[24] B. Peng, G. Chen, Y. Li, et al., Anal. Chem. 94 (2022) 11159–11167.
[25] H.W. Liu, X.X. Hu, K. Li, et al., Chem. Sci. 8 (2017) 7689–7695.
[26] J. Huang, C. Zhang, X. Wang, et al., Angew. Chem. Int. Ed. 62 (2023) e202303982.
[27] J. Miao, Y. Huo, G. Yao, et al., Angew. Chem. Int. Ed. 61 (2022) e202201815.
[28] Y. Luo, Z. Zeng, T. Shan, et al., Theranostics 12 (2022) 3610–3627.
[29] X. Zhou, H. Li, C. Shi, et al., Biomaterials 253 (2020) 120089.
[30] Q. Zhao, G. Qing, J. Yu, et al., Chin. Chem. Lett. 35 (2024) 108535.
[31] Y. Chen, X. Zhao, T. Xiong, et al., Sci. China Chem. 64 (2021) 808–816.
[32] C. Zhao, W. Sun, B. Tan, et al., Sens. Actuat. B: Chem. 382 (2023) 133502.
[33] Y. Xu, H. Chen, S. Xu, et al., ACS Sens. 7 (2022) 1361–1371.
[34] Q. Xu, Y. Ji, M. Chen, et al., Photochem. Photobiol. Sci. 20 (2021) 501–512.
[35] G. Cheng, J. Xing, Z. Pi, et al., Chin. Chem. Lett. 30 (2019) 656–659.
[36] C. Yan, Z. Guo, W. Chi, et al., Nat. Commun. 12 (2021) 3869.